A bi-annual journal published by the Faculty of Science, University of Lagos, Nigeria
http://jsrd.unilag.edu.ng/index.php/jsrd

Green synthesis of palladium nanoparticles using various capping agents for catalytic application

Ayorinde O. Nejo,[1*] Ademola J. Adetona,[1,2] and Sekinat O. Odumosu[1]
[1]Chemistry Department, Faculty of Science, University of Lagos, Nigeria
[2]School of Chemical, Materials and Biological Engineering, the University of Sheffield, United Kingdom. S1 3JD
Corresponding author: funaina2014@gmail.com

(Received 10 January 2025/Revised 12 April 2025/Accepted 16 April 2025)

Abstract

The demand for green chemistry approaches in nanotechnology has driven the development of environmentally benign methods for synthesizing metal nanoparticles. We investigate the green synthesis of palladium nanoparticles (Pd NPs) using plant extracts as eco-friendly capping and reducing agents. White onion (*Allium cepa*), turmeric (*Curcuma longa*), ginger (*Zingiber officinale*), and garlic (*Allium sativum*) extracts were investigated as capping agents for the synthesis of Pd NPs. The Pd NPs were characterized using FTIR and UV-Vis spectroscopy. For the FTIR results, there were shifts in the peaks after the synthesis of nanoparticles from the various extracts which ranged from 3276cm^{-1} – 3259cm^{-1} ; 2962cm^{-1} -2885cm^{-1}; 1627-1631cm^{-1} for OH and CH stretching, NH bond. While the UV results ranged from 196–424nm depending on the phytochemicals present in the extract. The functional groups in the plant and root extracts play a significant role in reducing and stabilizing Pd NPs, promoting nanoparticles with unique optical properties that offer a sustainable alternative to conventional chemical synthesis, yielding Pd NPs with promising catalytic applications in Buchwald-Hartwig animation reaction. Using abundant plant extracts presents an efficient, low-cost, and environmentally friendly approach to nanoparticle synthesis.

Keywords: Buchwald-Hartwig amination reaction, Green synthesis, Palladium nanoparticles, FTIR

1.0 Introduction

In recent years, there has been a growing interest in the production of environmentally benign or "green" methods for the synthesis of metal and metal oxide nanoparticles, such as Ti/TiO_2 (Aravind *et al.*, 2021; Dimo *et al.,* 2024; Dimo *et al.*, 2025), Ni/NiO (Ahmed *et al.,* 2022; Nejo *et al.*, 2024, Panadian *et al.*, 2015) , Pd/PdO (Mahnaz., 2019; Phan *et al,*, 2024; Sheny *et al.*, 2012). Green synthesis routes emphasize using abundant, non-toxic, renewable, and sustainable resources to reduce the environmental impact of metal/metal oxide nanoparticle production. The demand for sustainable nanotechnologies is increasing, and benign methods of preparing metal/metal oxide nanoparticles are needed (Ma'aruf *et al.*, 2024; Mahnaz , 2019; Sheny *et al,*, 2012).

Palladium (Pd) is widely used as a catalyst in coupling reactions, e.g. the Suzuki and Heck reactions and hydrogenation processes (Biffis *et al,*, 2018; Kharissova *et al.*, 2024). Pd has garnered attention in both homogeneous and heterogeneous catalytic systems. Palladium nanoparticles (Pd NPs) are catalysts in hydrogen storage (Alaqarbeh *et al.*, 2023), fuel cells (Stephen *et al.*, 2019), sensors (Zhaq, 2022), and environmental remediation applications (Alaqarbeh *et al.*, 2023; Omole, 2007). Pd NPs can facilitate various chemical processes, such as organic synthesis (Tao *et al.*, 2020), industrial catalysis (Van *et al.*, 2020), carbon-carbon bond formation (Gholinejad *et al.*, 2019), hydrogenation and oxidation reactions, making

them indispensable catalysts (Zhao *et al.*, 2021). Their size, large surface area and high surface energy contribute to their catalyst effectiveness. The high surface-to-volume ratio of Pd NPs has attracted great interest in enhancing catalytic activity. In catalysis, the high surface area of Pd NPs enhances catalytic reactions, resulting in the efficacy of the nanoparticle catalyst. In preparing palladium nanoparticles, various reducing agents such as sodium borohydride ($NaBH_4$), hydrazine (N_2H_4), and ascorbic acid are commonly used, which are expensive and require high energy input. In addition, these reducing agents are not eco-friendly and often contaminate the Pd NPs produced, limiting their catalytic performance and practical applications. The conventional methods of synthesizing palladium nanoparticles present challenges due to the environmental and economic costs linked to toxic reagents and significant energy consumption (Joudeh *et al.*, 2022; Salda *et al.,* 2015).

One benign method for the green synthesis of palladium nanoparticles involves using plant extracts as reducing and capping agents (Veisi *et al.*, 2014; Kanchana *et al.*, 2010; Qazi *et al.*, 2016). Plant extracts are rich in biomolecules, such as polyphenols, alkaloids, terpenoids, and proteins, which can effectively reduce metal ions to their nanoparticle form (Adeyemi *et al.*, 2022; El seedi *et al.*, 2019; Ovais *et al.*, 2018; Shafey *et al.*, 2020). These biomolecules also act as stabilizing agents, preventing the agglomeration of nanoparticles and helping to control their size and morphology. This method is advantageous because it is simple, cost-effective, scalable, and avoids harmful chemicals. Plant-based green synthesis reduces the environmental impact of nanoparticle production and results in nanoparticles that are free of contamination and have well-defined physical and chemical properties. Numerous studies have demonstrated the successful green synthesis of Pd NPs using various plant extracts, *Coleus amboinicus* (Bathula *et al.*, 2020), *Lagerstroemia speciose* (Garole *et al.*, 2019), *Thymbra Spicata* (Sepideh *et al.*, 2018), *Pimpinella tirupatiensis* (Palajoma *et al.*, 2017), *Chrysophyllum cainito* (Majumdar *et al.*, 2017), *Fenugreek tea* (Koduru *et al.,* 2017), *Glycyrrhiza glabra* (Veisi *et al.,* 2017), *Ocimum sanctum* (Manashi *et al.*, 2019), *Euphorbia granulate* (Nasrollahzadeh *et al.*, 2016), *Origanum vulgare L* (Shaik *et al.*, 2017) and *Terminalia arjuna* (Garai .*et al.*, 2018). There has been limited to no exploration of using fresh fruits such as onion, turmeric, ginger, and garlic. In this study, Pd nanoparticles were synthesised using white onion (*Allium cepa*), turmeric (*Curcuma longa*), ginger (*Zingiber officinale*), and garlic (*Allium sativum*) as capping/reducing agents, and to evaluate its potential as a catalyst in the Buchwald Hartwig animation reaction.

2. Experimental methods

2.1 Preparation of capping/reducing agents

A 100 g fresh plant roots (*Allium cepa*—white onion, *Curcuma longa*—turmeric, *Zingiber officinale*—ginger, and *Allium sativum*—garlic) were weighed, washed, and oven-dried at 60 °C for 48 hr. The dried roots were ground to a fine powder (*Allium sativum* (Figure 1a), *Zingiber officinale* (Figure 2a), *Curcuma longa* (Figure 3a) and *Allium cepa* (Figure 4a)), sieved, and stored in an airtight container at room temperature. For extraction, 2 g of each powdered plant was dissolved in 50 mL of distilled H_2O, boiled in a water bath for 1 hour, and then cooled. The solutions were filtered through 5 µm filter paper, and the extracts were stored for the green synthesis of Pd NPs.

2.2 Green syntheses of Pd nanoparticles: 0.18 g $PdCl_2$ was dissolved in distilled H_2O, diluted to 100 ml in a standard flask, and then stored to synthesise Pd NPs. 20 mL of extract was measured and mixed with 40 mL of the prepared $PdCl_2$ solution in a round-bottom flask. A stirrer bar was added, and the flask was clamped to a retort stand. The flask was covered with foil paper and placed on a magnetic stirrer set to 30°C at 250 rpm for 24 hours to maintain darkness. After this period, a dark brown colouration was observed, indicating the formation of Pd NPs solution (Ramesh *et al,*, 2012). The solution was centrifuged at 1500 rpm for 10 minutes, then washed with distilled H_2O, methanol, and acetone to remove biomolecules. The Pd NPs were dried and stored for characterization.

Figure 1: (a) *Allium sativum* (garlic) powder (b) *Allium sativum* extract (c) Pd nanoparticles solution using *Allium sativum* extract and $PdCl_2$ solution after 24 hr.

Figure 2: (a) *Zingiber officinale* (ginger) powder (b) *Zingiber officinale* extract (c) Pd nanoparticles solution using *Zingiber officinale* extract and $PdCl_2$ solution after 24 hr.

Figure 3: (a) *Curcuma longa* (turmeric) powder (b) *Curcuma longa* extract (c) Pd nanoparticles solution using *Curcuma longa* extract and $PdCl_2$ solution after 24 hr

Figure 4: (a) *Allium cepa* (white onion) powder (b) *Allium cepa* extract (c) Pd nanoparticles solution using *Allium cepa* extract and $PdCl_2$ solution after 24 hr.

3.0 Characterization of the Pd NPs: The chemical and optical properties of the Pd NPs were studied using spectroscopic techniques, vibrational mode of the capping/reducing agents (ginger, garlic, turmeric, and white onion extracts) and the bio-reduction of the Pd NPs (the extract-mixture was centrifuged at 1500 rpm for 10 minutes to separate the Pd^{2+} NPs from proteins and other components in the mixture) were studied by Bruker FTIR spectrometer and the electronic transition was investigated by the UV Shimadzu series.

4.0 Results

4.1 FTIR spectra of *Allium sativum* (garlic) and Pd NPs mediated by *Allium sativum*

Figure 5a shows the spectrum of garlic extract without palladium chloride, while Figure 5b shows the spectrum after bio-reduction with $PdCl_2$. The FT-IR spectra of garlic extract (Figure 5a) reveal the presence of Allicin, indicated by peaks at 1040 cm^{-1} (S=O) and 1307 cm^{-1} (S group), the main component of garlic *(*Rajam *et al*,2012*)*. Additionally, broad peaks at 3276 cm^{-1} and 2962 cm^{-1} correspond to -OH and -CH stretches, respectively, characteristic of non-structural sucrose and fructose. The sharp peak at 1627 cm^{-1} is attributed to N-H bond in primary amines, while the peak at 1396 cm^{-1} suggests C-N stretching in aromatic amines. After synthesising Pd NPs (Figure 5b), shifts were observed at 3276-3272 cm^{-1}, 2962-2885 cm^{-1}, 1627-1631 cm^{-1}, 1564-1537 cm^{-1}, 1396-1390 cm^{-1}, and 923-919 cm^{-1}, indicating the involvement of hydroxyl groups, primary and aromatic amines, and esters in the nanoparticle formation. The stretching between 763 cm^{-1} and 833 cm^{-1} confirmed the presence of residual Cl_2, while peaks at 599 cm^{-1}, 561 cm^{-1}, and 2362 cm^{-1} indicate Pd NPs bonding with oxygen from the garlic extract.

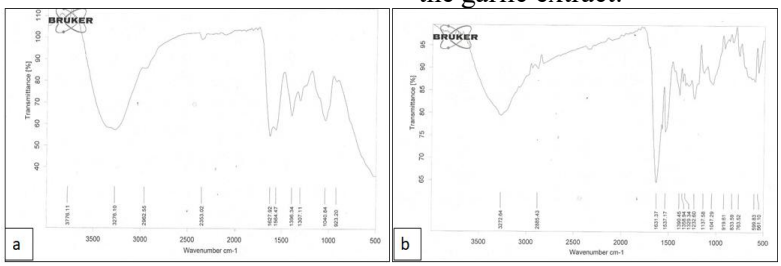

Figure 5: FTIR spectra of (a) *Allium sativum* (garlic), (b) Pd NPs mediated by *Allium sativum* (garlic)

4.2 FTIR spectra of *Zingiber officinale* and Pd NPs mediated by *Zingiber officinale*

Figure 6a shows the spectrum of ginger extract without palladium chloride, while Figure 6b shows the spectrum after bio-reduction with $PdCl_2$. The FTIR analysis (Figure 6a) reveals distinct bands, including one at 3776 cm^{-1} corresponding to O-H stretching in H-bonded alcohols and phenols, a broad peak at 3276 cm^{-1} for O-H stretching in carboxylic acids, a peak at 1627 cm^{-1} for N-H bending in primary amines, and peaks at 1396 cm^{-1} and 1307 cm^{-1} for C-N stretching in aromatic amines. Additionally, a peak at 1040 cm^{-1} indicates the presence of esters. After synthesising palladium nanoparticles (Figure 6b), noticeable shifts in these peaks (from 3276 to 3259 cm^{-1}, 1627 to 1630 cm^{-1}, 1401 to 1396 cm^{-1}, and 1040 to 1024 cm^{-1}) suggest that hydroxyl groups, primary amines, aromatic amines, and esters from ginger

rhizome were involved in the synthesis process. These functional groups, primarily derived from water-soluble heterocyclic compounds in ginger, likely include alkaloids and flavonoids, which may have acted as capping agents for forming ginger-capped palladium nanoparticles *(*Geetha *et al.*, 2014*)*.

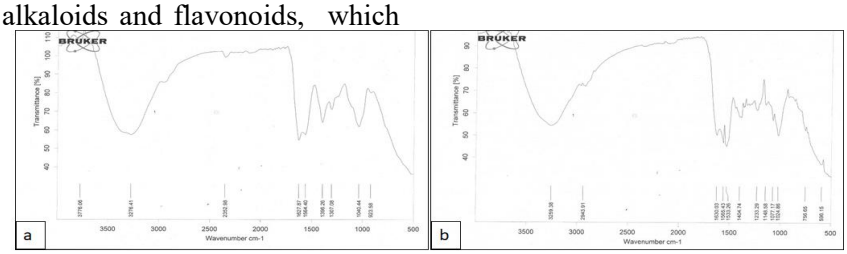

Figure 6: FTIR spectra of (a) *Zingiber officinale* (ginger), (b) Pd NPs mediated by *Zingiber officinale*

4.3 FTIR spectra of *Curcuma longa* (turmeric) and Pd NPs mediated by *Curcuma longa*

Figure 7a shows the spectrum of turmeric extract without palladium chloride, while Figure 7b shows the spectrum after bio-reduction with $PdCl_2$. In Figure 7a, a broad peak at 3293 cm^{-1} indicates the presence of O-H hydroxyl groups, while the peak at 2942 cm^{-1} corresponds to aliphatic C-H, and the 1622 cm^{-1} peak is attributed to carbonyl (-C=O) stretching. Additionally, absorption peaks at 994 cm^{-1}, 923 cm^{-1}, and 1026 cm^{-1} correspond to C-N stretching of amines and C-O or C-O-C groups. These functional groups, including -C-O-C, -C-O, and amide bonds from alkaloids, flavones, and proteins in the extract, serve as capping nanoparticle ligands. In Figure 7b, the strong bands at 3198 cm^{-1} are due to bonded O-H or amine (-NH) groups, and the peak at 2884 cm^{-1} is linked to aliphatic C-H. The stretch between 783 cm^{-1} and 763 cm^{-1} indicates residual Cl_2, while broad peaks at 612 cm^{-1}, 608 cm^{-1}, and 2358 cm^{-1} suggest Pd NPs bonding with oxygen from hydroxyl groups in turmeric. These functional groups likely participated in the nanoparticle synthesis *(*Shameli *et al.*, 2012*)*.

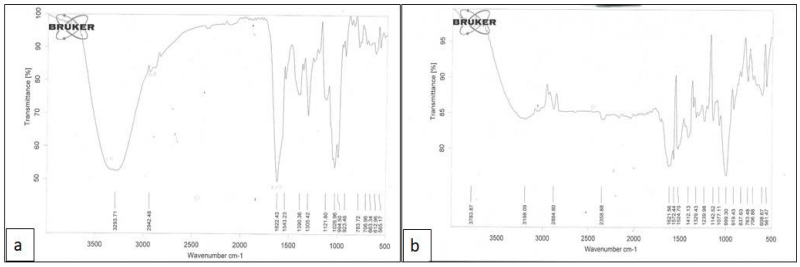

Figure 7: FTIR spectra of (a) *Curcuma longa* (turmeric), (b) Pd NPs mediated by *Curcuma longa*

4.4 FTIR spectra of *Allium cepa* (white onion) and Pd NPs mediated by *Allium cepa*

Figure 8a shows the white onion extract without palladium chloride, while Figure 8b shows the spectrum after bio-reduction with $PdCl_2$. The FT-IR spectra of white onion extract (Figure 8a) reveal a distinctive peak at 1635 cm^{-1}, attributed to the C-C stretch of phenyl, a key component in the polyphenolic compounds found in Allium plants. The peak at 1397 cm^{-1} is due to asymmetric deformation. Additionally, broad -OH and $-CH_2$ antisymmetric stretches from lipids are observed at 3296 cm^{-1} and 2934 cm^{-1}. The 1635 cm^{-1} peak is associated with N-H stretching of proteins and O-H stretching from carbohydrates and water, while the sharp peak at 1032 cm^{-1} corresponds to strong sulfoxide stretching. After the synthesis of palladium nanoparticles (Figure 8b), five major peaks emerged. The O-H group (previously represented by a peak at 2919 cm^{-1}) disappeared, and a new peak at 2358 cm^{-1} appeared, which was absent in the original extract. Shifts from 2934 to 2919 cm^{-1}, 1631 to 1616 cm^{-1}, 1397 to 1369 cm^{-1}, and 1032 to 1055 cm^{-1} suggest the involvement of aliphatic sp^3-CH, N-H from primary amines, C-N stretching of aromatic amines, and sulfoxide groups, confirming the successful formation of Pd NPs. Stretching between 777 cm^{-1} and 816 cm^{-1} indicates the presence of residual Cl_2 *(*Piermatti *et al*, 2021*)*.

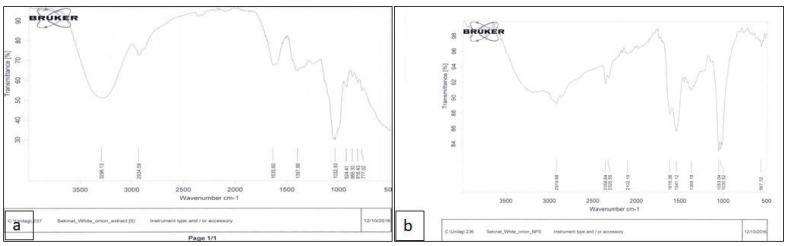

Figure 8: FTIR spectra of (a) *Allium cepa* (white onion), (b) Pd NPs mediated by *Allium cepa*

4.5 UV Visible spectra

The formation of metal nanoparticles by reducing the aqueous metal ions during the extracts' exposure is easily followed by UV–Vis spectroscopy. The UV-Vis absorbance spectra of Pd NPs synthesised using extracts from *Allium cepa* (white onion), *Curcuma longa* (turmeric), *Zingiber officinale* (ginger), and *Allium sativum* (garlic) are shown in Figure 9 (a-d). Each spectrum shows a distinct absorption peak based on the extract used. For *Allium cepa* (white onion), the Pd NPs exhibited an absorption peak at 424 nm (Figure 9a), suggesting interactions between the nanoparticle surface and the onion extract. Pd NPs from *Curcuma longa* (turmeric) showed a peak at 384 nm (Figure 9b), indicating a blue shift compared to *Allium cepa*, which may be due to differences in nanoparticle size or surface chemistry influenced by turmeric's phytochemicals. The Pd NPs synthesised with *Zingiber officinale* (ginger) had an absorption peak at 196 nm (Figure 9c) (blue-shifted than the other extracts), suggesting distinct nanoparticle characteristics *(*Bindhu *et al.*, 2013; Piermatti *et al*,2021 *)*. The Pd NPs from *Allium sativum* (garlic) peaked at 422 nm (Figure 9d), similar to *Allium cepa*, indicating that these nanoparticles share similarities, likely due to both plants belonging to the *Amaryllidaceae* family *(*Piermatti *et al.*, 2021; Shankar *et al.*. 2004*)*. The variations in absorption peaks reflect the influence of the extracts' phytochemical properties on the optical properties of the Pd NPs. These shifts suggest differences in the size, morphology, and surface capping of the nanoparticles, with results aligning with findings in previous studies.

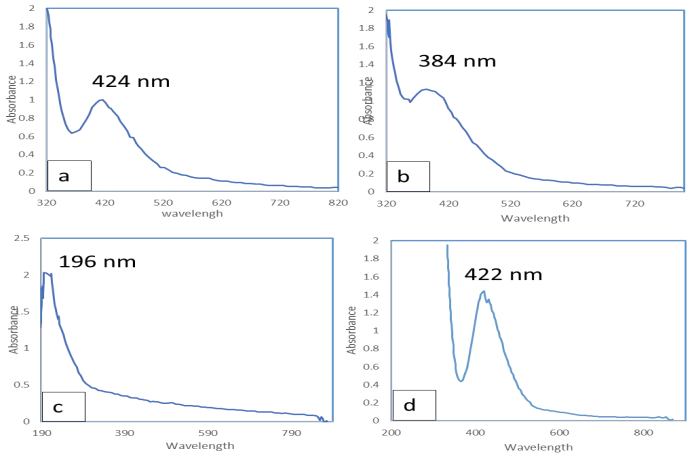

Figure 9: UV-Vis spectra of Pd NPs green synthesised by (a) *Allium cepa* (white onion) extract, (b) *Curcuma longa* (turmeric) extract, (c) *Zingiber officinale* (ginger) extract, (d) *Allium sativum*(garlic).

4.6 Band Gap Energy

The band gap energy depicts the wavelength of light a material can absorb. Compounds with larger band gaps absorb light at shorter wavelengths, corresponding to higher energy and compounds with smaller band gaps absorb light at longer wavelengths, indicating lower energy absorption. The band gaps of Pd NPs

synthesised from *Allium cepa* (white onion), *Curcuma longa* (turmeric), *Zingiber officinale* (ginger), and *Allium sativum* (garlic) extracts were calculated using equation 1, as shown in Table 1. The wavelength was obtained from the UV-visible spectra.

$E = \frac{hc}{\lambda}$ ..... (1).

where λ = wavelength, C = speed of light and h = Planck's constant = 6.626 x 10^{-34} Js.

Table: Band gap energy of Pd NPs from different fruit and root extracts.

Fruit Extracts	Wavelength (λ)	Planck's constant (Js)	Speed of Light (m/s)	Pd NPs Band Gap Energy (J)	Pd NPs Band Gap Energy (eV)
Allium cepa	424 x 10^{-9}	6.626 x 10^{-34}	3 x 10^{8}	4.69 x 10^{-19}	2.93
Curcuma longa	384 x 10^{-9}	6.626 x 10^{-34}	3 x 10^{8}	5.18 x 10^{-19}	3.23
Zingiber officinale	196 x 10^{-9}	6.626 x 10^{-34}	3 x 10^{8}	1.01 x 10^{-18}	9.92
Allium sativum	422 x 10^{-9}	6.626 x 10^{-34}	3 x 10^{8}	4.71 x 10^{-19}	2.94

5.0 Catalytic application of Pd NPs in Buchwald Hartwig Animation Reaction

The Buchwald-Hartwig amination is a palladium-catalysed organic reaction that forms carbon-nitrogen bonds by coupling an aryl halide with an amine in a strong base (e.g. NaOH). The reaction starts with the oxidative addition of the aryl halide to the Pd NPs catalyst, followed by the amine coordinating with the Pd NPs complex, and the base deprotonates the amine, forming an amide. The amide then displaces the halide from the palladium complex, and reductive elimination occurs, yielding the aryl amine product and regenerating the palladium catalyst *(*Sakata *et al.*, 2021; Sherwood *et al.*, 2019*)*.

In the next phase, two Pd NPs, synthesised from *Curcuma longa* (turmeric) and *Zingiber officinale* (ginger) extracts, were used as catalysts in Buchwald-Hartwig amination reactions. Three different reactions were studied, each conducted for 24 hours at room temperature using 0.010–0.013 g of the synthesised Pd NPs. The results demonstrated the effectiveness of Pd NPs as efficient catalysts, highlighting their potential for industrial applications.

5.1 FORMATION OF 1-PHENYL PYRROLIDINE

A 5 mL of toluene was measured in a round-bottomed flask, adding 1mmol (0.157 g) of bromobenzene and 1mmol (0.071 g) of pyrrolidine. A 2 mmol (0.424 g) of K_3PO_4 was added as a base, along with 0.010 g of *Curcuma longa* (turmeric) extract Pd NPs as the catalyst. An additional 2 mL of toluene was added to the solution, which was then placed in a sand bath and refluxed at 150°C using an air condenser for 24 hours, as shown in equation 2. The reaction progress was monitored using a TLC plate. After 24 hours, the reaction was worked up by washing with dichloromethane, n-hexane, and ethyl acetate. The mixture was filtered after adding ethyl acetate, and the filtrate was covered with aluminium foil to allow the ethyl acetate to evaporate.

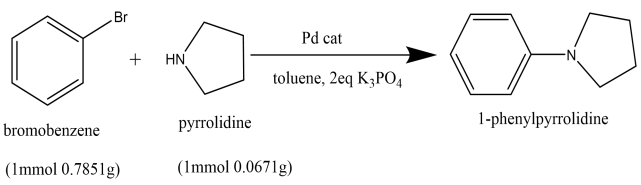

Equation 2. Formation of 1-phenyl pyrrolidine

5.1.1 FT-IR SPECTRA FOR 1-PHENYL PYRROLIDINE USING GINGER Pd NPs

The FTIR spectrum of 1-phenyl pyrrolidine shows characteristic absorption bands that confirm its structure, Figure 10. Aromatic C-H stretches around 3105 cm^{-1}, while the pyrrolidine ring's C-H stretches are near 3020 cm^{-1}. Aromatic C=C stretches occur at 1617 cm^{-1}, and C-N stretching vibrations are around 1080 cm^{-1}. Compared to pyrrolidine, which has an N-H stretch at 3266 cm^{-1} and sp^3-CH stretches at 2957 cm^{-1} and 2867 cm^{-1}, the phenyl group in 1-phenylpyrrolidine shifts these frequencies due to conjugation effects. These peaks can help monitor product formation in the Buchwald-Hartwig amination reaction *(*Piermatti *et al*, 2021*)*.

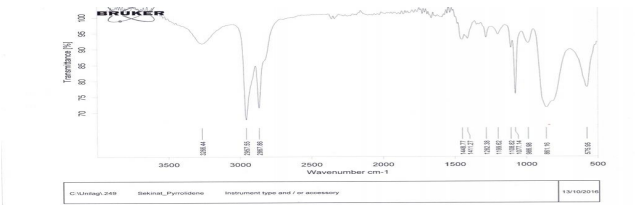

Figure 10: FTIR spectra of 1-phenyl pyrrolidine

5.2 PREPARATION OF 1-(2,4-DINITROPHENYL) PYRROLIDINE USING GINGER Pd NPs

In a round-bottomed flask, 10 mL of toluene was combined with 1mmol (0.2025 g) of 1-chloro-2,4-dinitrobenzene, 1 mmol (0.071 g) of pyrrolidine, and 2mmol (0.424 g) of K_3PO_4 as the base. 0.012 g of ginger-synthesized Pd NPs was added as a catalyst, as shown in Equation 3. The reaction mixture was then air-refluxed at 150°C for 24 hours, with progress monitored using TLC.

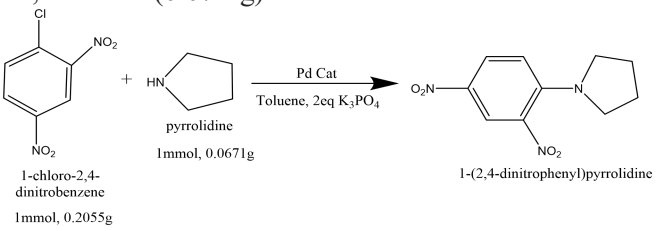

Equation 3. Formation of 1-(2,4-dinitrophenyl) pyrrolidine.

5.2.1 FTIR SPECTRA OF 1-(2,4-DINITROPHENYL) PYRROLIDINE USING GINGER Pd NPs

The FTIR analysis indicates the disappearance of the secondary N-H band from pyrrolidine, suggesting reaction completion, Figure 11. Peaks confirm the presence of sp^2-CH at 2862 cm^{-1}, 2919 cm^{-1}, and 1607 cm^{-1}, replacing the sp^3 stretches seen in pyrrolidine at 2957 cm^{-1} and 2867 cm^{-1}. Tri-substituted C-H bending appears at 740 cm^{-1} and 721 cm^{-1}. Strong asymmetric and symmetric -NO_2 stretches are observed at 1523 cm^{-1} and 1320 cm^{-1}, respectively. The aliphatic tertiary amine C-N stretch at 1140 cm^{-1} confirms the successful formation of the desired product.

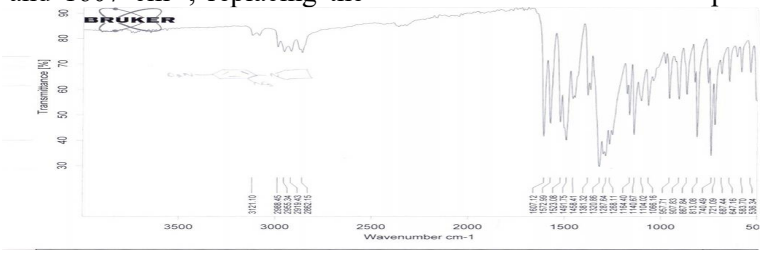

Figure 11: FTIR spectra of 1-(2,4-dinitrophenyl) pyrrolidine using ginger palladium nanoparticles

5.3 PREPARATION OF 1-(4-NITROPHENYL) PYRROLIDINE USING TUMERIC Pd NPs

In a round-bottomed flask, 10 mL of toluene was mixed with 1mmol (0.424 g) of 1-fluoro-4-nitrobenzene, 1 mmol (0.071 g) of pyrrolidine, and 2 mmol (0.424 g) of K_3PO_4 as the base. 0.010 g of turmeric-synthesized Pd NPs was added as the catalyst, as shown in equation 4. The reaction mixture was then air-refluxed at 150°C for 24 hours, with its progress monitored using TLC.

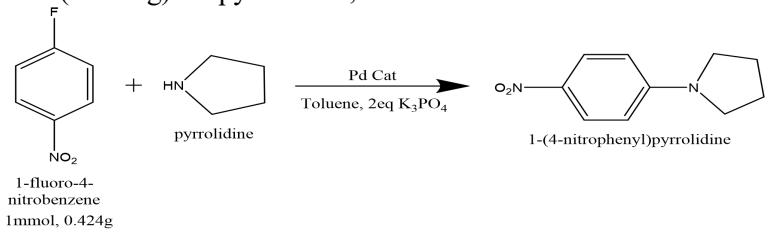

Equation 4. Formation of 1-(4-nitrophenyl) pyrrolidine

5.3.1 FTIR SPECTRA OF 1-(4-NITROPHENYL) PYRROLIDINE USING TUMERIC Pd NPs

The FTIR spectrum shows the disappearance of the secondary N-H band from pyrrolidine, confirming the reaction, Figure 12. Peaks at 2858 cm^{-1} and 2918 cm^{-1} indicate the presence of sp^2-CH, while di-substituted C-H bending is observed at 817 cm^{-1} and 751 cm^{-1}. Strong -NO_2 stretching is noted at 1430 cm^{-1} and 1519 cm^{-1}. The medium aliphatic tertiary amine C-N stretch at 1106 cm^{-1} further confirms that the reaction was completed, and the product was successfully formed *(*Frindy *et al.*, 2015*)*.

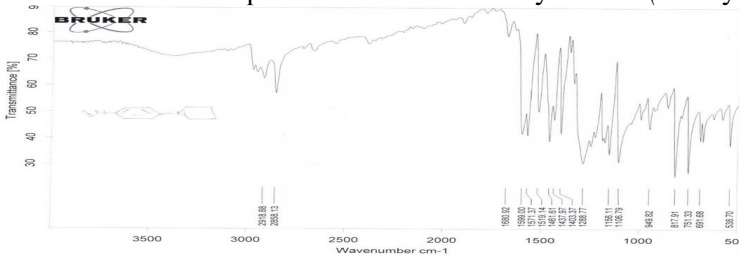

Figure 12: FTIR spectra of 1-(4-nitrophenyl) pyrrolidine using Turmeric Pd NPs

5.4 PREPARATION OF 1-(2,4-DINITROPHENYL) PYRROLIDINE USING TUMERIC Pd NPs

In a round-bottomed flask, 10 mL of toluene was mixed with 1mmol (0.2025 g) of 1-chloro-2,4-dinitrobenzene, 1mmol (0.071 g) of pyrrolidine, and 2 mmol (0.424 g) of K_3PO_4 as the base. Next, 0.012 g of turmeric-synthesized Pd NPs was added as the catalyst, as shown in Equation 5. The reaction mixture was then air-refluxed at 150°C for 24 hours, with progress monitored using TLC.

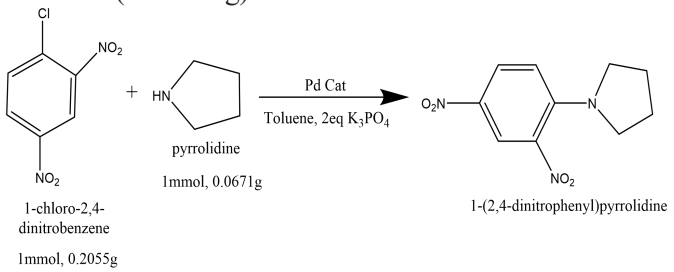

Equation 5. Formation of 1-(2,4-dinitrophenyl) pyrrolidine.

5.4.1 FTIR SPECTRA OF 1-(2,4-DINITROPHENYL) PYRROLIDINE USING TUMERIC Pd NPs

The FTIR result shows that the secondary N-H band from pyrrolidine is still present, indicating an incomplete reaction, Figure 13. Peaks at 2862 cm^{-1}, 2919 cm^{-1}, and 1607 cm^{-1} confirm the

presence of sp^2-CH, replacing the sp^3-CH stretches observed in pyrrolidine at 2957 cm^{-1} and 2867 cm^{-1}. Tri-substituted C-H bends are observed at 740 cm^{-1} and 720 cm^{-1}. Strong asymmetric -NO_2 stretching is seen at 1522 cm^{-1}, and symmetric -NO_2 appears at 1321 cm^{-1}. The medium C-N stretch at 1139 cm^{-1} suggests the reaction is incomplete, and further stirring may have been needed for product formation *(*Veisi *et al.*, 2015*)*.

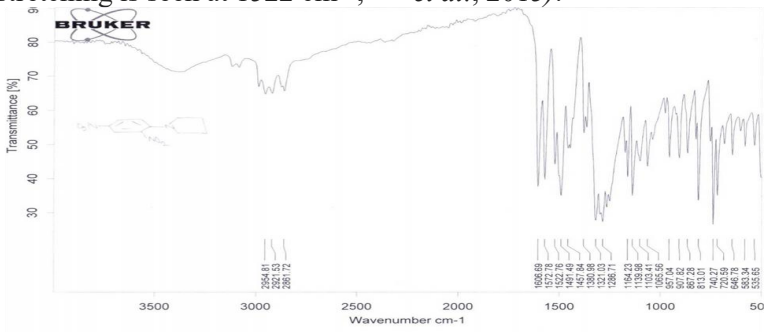

Figure 13: FTIR spectra of 1-(2,4-Dinitrophenyl) Pyrrolidine using turmeric Pd NPs

6.0 Conclusion

This study successfully synthesised palladium nanoparticles (Pd NPs) using green methods with polyphenolic antioxidants from turmeric, ginger, garlic, and white onion extracts. The bio-reduction of Pd (II) ions was achieved under dark conditions at room temperature, confirmed by UV-Vis and FT-IR spectroscopy. The resulting Pd NPs had band gap energies ranging from 2.93 eV to 9.92 eV. Ginger and turmeric Pd NPs demonstrated effective catalytic activity in Buchwald-Hartwig animation without requiring a ligand. Using plant extracts as reducing and capping agents, this eco-friendly approach presents a sustainable alternative to traditional nanoparticle synthesis. The study highlights the potential of these green-synthesized Pd NPs for industrial catalysis and environmental applications, promoting the use of renewable, non-toxic resources in nanotechnology.

References

Adeyemi, J. O.; Oriola, A. O.; Onwudiwe, D. C.; Oyedeji, A. O.(2022) Plant Extracts Mediated Metal-Based Nanoparticles: Synthesis and Biological Applications. *Biomolecules*, *12* (5), 627. https://doi.org/10.3390/biom12050627.

Ahmad, W.; Chandra Bhatt, S.; Verma, M.; Kumar, V.; Kim, H. A (2022)Review on Current Trends in the Green Synthesis of Nickel Oxide Nanoparticles, Characterizations, and Their Applications. *Environmental Nanotechnology, Monitoring & Management* , *18*, 100674. https://doi.org/10.1016/j.enmm.2022.100674.

Alaqarbeh, M.; Adil, S. F.; Ghrear, T.; Khan, M.; Bouachrine, M.; Al-Warthan, A.(2023) Recent Progress in the Application of Palladium Nanoparticles: A Review. *Catalysts*, *13* (10), 1343. https://doi.org/10.3390/catal13101343.

Aravind, M.; Amalanathan, M.; Mary, M. S. M.(2021) Synthesis of TiO_2 Nanoparticles by Chemical and Green Synthesis Methods and Their Multifaceted Properties. *SN Applied Sciences* , *3* (4). https://doi.org/10.1007/s42452-021-04281-5.

Bathula, C.; K, S.; Kumar K, A.; Yadav, H.; Ramesh, S.; Shinde, S.; Shrestha, N. K.; Mallikarjuna, K.; Kim, H.(2020) Ultrasonically Driven Green Synthesis of Palladium Nanoparticles by Coleus Amboinicus for Catalytic Reduction and Suzuki-Miyaura Reaction. *Colloids and Surfaces B: Biointerfaces*, *192*, 111026. https://doi.org/10.1016/j.colsurfb.2020.111026.

Biffis, A.; Centomo, P.; Del Zotto, A.; Zecca, M. (2018) Pd Metal Catalysts for Cross-Couplings and Related Reactions in the 21st Century: A Critical Review. *Chemical Reviews* *118* (4), 2249–2295. https://doi.org/10.1021/acs.chemrev.7b00443.

Bindhu, M. R.; Umadevi, M. (2013)Synthesis of Monodispersed Silver Nanoparticles Using Hibiscus Cannabinus Leaf Extract and Its Antimicrobial Activity. *Spectrochimica Acta Part A: Molecular and Biomolecular*

Spectroscopy, *101*, 184–190. https://doi.org/10.1016/j.saa.2012.09.031.

Dimo, S. N.; Obidi, O. F.; Nejo, A. O.; Olaleru, S. A.; Ejidike, I. P.; Adetona, A. J.(2024) Biofabrication, Spectroscopic, and Photocatalytic Studies of Titania Nanoparticles Mediated by *Proteus Mirabilis* Strain NG-ABK-32 for Smart Applications. *Smart Science* , *12* (2), 373–386. https://doi.org/10.1080/23080477.2024.2338651.

Dimo, S. N.; Obidi, O. F.; Nejo, A. O.; Olaleru, S. A.; Ejidike, I. P.; Adetona, A. J. (2025) Preparation of Nanosized TiO_2 in the Presence of Bacteria Bacillus Paralicheniformis and Its Photocatalytic Properties in the Process of Decolorization of Dyes. *Theoretical and Experimental Chemistry*. https://doi.org/10.1007/s11237-025-09821-3.

El-Seedi, H. R.; El-Shabasy, R. M.; Khalifa, S. A. M.; Saeed, A.; Shah, A.; Shah, R.; Iftikhar, F. J.; Abdel-Daim, M. M.; Omri, A.; Hajrahand, N. H.; Sabir, J. S. M.; Zou, X.; Halabi, M. F.; Sarhan, W.; Guo, W.(2019) Metal Nanoparticles Fabricated by Green Chemistry Using Natural Extracts: Biosynthesis, Mechanisms, and Applications. *RSC Advances* , *9* (42), 24539–24559. https://doi.org/10.1039/c9ra02225b.

Frindy, S.; Primo, A.; Lahcini, M.; Mosto Bousmina; Garcia, H.; Abdelkrim El Kadib.(2015) Pd Embedded in Chitosan Microspheres as Tunable Soft-Materials for Sonogashira Cross-Coupling in Water–Ethanol Mixture. *Green Chemistry*, *17* (3), 1893–1898. https://doi.org/10.1039/c4gc02175d.

Garai, C.; Sk Md Hasan; Abir, C. B; Subrata, G; S, K, Panja; and Braja G. B.(2018) Green Synthesis of Terminalia Arjuna-Conjugated Palladium Nanoparticles (TA-PdNPs) and Its Catalytic Applications., *8* (4), 465–472. https://doi.org/10.1007/s40097-018-0288-z.

Garole, V. J.; Choudhary, B. C.; Tetgure, S. R.; Garole, D. J.and Borse, A. U. (2019) Palladium Nanocatalyst: Green Synthesis, Characterization, and Catalytic Application. *International Journal of Environmental Science and Technology*, *16* (12), 7885–7892. https://doi.org/10.1007/s13762-018-2173-1.

Geetha, N.; Geetha, T.; Manonmani, P. and Thiyagarajan, M.(2014) Green Synthesis of Silver Nanoparticles Using Cymbopogan Citratus (Dc) Stapf. Extract and Its Antibacterial Activity. *Australian Journal of Basic and Applied Sciences*, *8* (3), 324–331.

Gholinejad, M.; Naghshbandi, Z. and Nájera, C. (2019)Carbon-Derived Supports for Palladium Nanoparticles as Catalysts for Carbon-Carbon Bonds Formation. *ChemCatChem***2**, *11* (7), 1792–1823. https://doi.org/10.1002/cctc.201802101.

Joudeh, N.; Athanasios Saragliadis; Koster, G.; Pavlo Mikheenko; and Linke, D.(2022) Synthesis Methods and Applications of Palladium Nanoparticles: A Review., *4*. https://doi.org/10.3389/fnano.2022.1062608.

Kanchana, A.; Devarajan, S.; Ayyappan, S. R.(2010) Green Synthesis and Characterization of Palladium Nanoparticles and Its Conjugates from Solanum Trilobatum Leaf Extract. *Nano-Micro Letters* , *2* (3), 16–176. https://doi.org/10.1007/bf03353637.

Kharissova, O. V.; Kharisov, B. I.; Oliva González, C. M.; Méndez, Y. P. and López, I. Greener Synthesis of Chemical Compounds and Materials. *Royal Society Open Science*, *6* (11), 191378. https://doi.org/10.1098/rsos.191378.

Koduru Mallikarjuna; Chinna Bathula; Kezia Buruga; Shrestha, N. K.; Noh, Y.-Y.; Kim, H. (2017) Green Synthesis of Palladium Nanoparticles Using Fenugreek Tea and Their Catalytic Applications in Organic Reactions. *Materials Letters*, *205*, 138–141. https://doi.org/10.1016/j.matlet.2017.06.081.

Ma'aruf, A. M,, Mustapha, S, G., Tailor, Muhammad, N. Sulaiman, and H. M, Usman.(2022) Sustainable Synthesis Strategies: Biofabrication's Impact on Metal and Metal Oxide Nanoparticles. - *African Journal of Environment and Natural Science Research (AJENSR)**2024,** 7 (11)*. https://dx.doi.org/10.52589/ajensr-jtfpyhuk .

Mahnaz, M. S. (2019 Highly Efficient of Cross-Coupling Reaction Supported Green Synthesized Palladium Nanoparticles Coated Natural Ligands as Heterogeneous Reusable Nanocatalyst. *DOAJ (DOAJ: Directory of Open Access Journals)*. https://doi.org/10.22052/jns.2019.04.009.

Majumdar, R.,Tantayanon, S.; and Bag, B. G.(2017) Synthesis of Palladium Nanoparticles with Leaf Extract of Chrysophyllum Cainito (Star Apple) and Their Applications as Efficient Catalyst for C–C Coupling and Reduction Reactions. *International Nano Letters* , *7* (4), 267–274. https://doi.org/10.1007/s40089-017-0220-4.

Manashi, S.; A. B. Neog, Boruah, P. K.; Das, M. R.; Pankaj B.,and Bora, U.(2019) Effect of Substrates on Catalytic Activity of Biogenic Palladium Nanoparticles in C–c Cross-Coupling Reactions. *ACS omega* , *4* (2), 3329–3340. https://doi.org/10.1021/acsomega.8b02697.

Nasrollahzadeh, M.; Mohammad Sajadi, S. (2016) Pd Nanoparticles Synthesized in Situ with the Use of Euphorbia Granulate Leaf Extract: Catalytic Properties of the Resulting Particles. *Journal of Colloid and Interface Science*, *462*, 243–251. https://doi.org/10.1016/j.jcis.2015.09.065.

Nejo, A. O.; Adetona, A. J. and Lawal, A.(2024) Green Synthesis of Nickel Oxide Nanoparticles and Its Application in the Degradation of Methyl Red. *Lafia Journal of Scientific and Industrial Research* , 54–60. https://doi.org/10.62050/ljsir2024.v2n2.328.

Omole, M. A.; K'Owino, I. O., and Sadik, O. A. (2007) Palladium Nanoparticles for Catalytic Reduction of Cr(VI) Using Formic Acid. *Applied Catalysis B: Environmental*, *76* (1-2), 158–167. https://doi.org/10.1016/j.apcatb.2007.05.018.

Ovais, M.; Khalil, A. T.; Islam, N. U.; Ahmad, I.; Ayaz, M.; Saravanan, M.; Shinwari, Z. K. and Mukherjee, S. (2018) Role of Plant Phytochemicals and Microbial Enzymes in Biosynthesis of Metallic Nanoparticles. *Applied Microbiology and Biotechnology* **2018**, *102* (16), 6799–6814. https://doi.org/10.1007/s00253-018-9146-7.

Palajonna, N.; B. K. Mandal and N.C. Sarada.(2017) Green Synthesis of Pd NPs from Pimpinella Tirupatiensis Plant Extract and Their Application in Photocatalytic Activity Dye Degradation. **2017**, *263*, 022013–022013. https://doi.org/10.1088/1757-899x/263/2/022013.

Pandian, C. J.; Palanivel, R. and Dhananasekaran, S. (2015) Green Synthesis of Nickel Nanoparticles Using Ocimum Sanctum and Their Application in Dye and Pollutant Adsorption. *Chinese Journal of Chemical Engineering*, *23* (8), 1307–1315. https://doi.org/10.1016/j.cjche.2015.05.012.

Phan, T. T. V. (2024)A Review of the Green Synthesis of Palladium Nanoparticles for Medical Applications. *Journal of Cluster Science*, *35* (6), 1915–1931. https://doi.org/10.1007/s10876-024-02634-9.

Piermatti, O.(2021) Green Synthesis of Pd Nanoparticles for Sustainable and Environmentally Benign Processes. *Catalysts*, *11* (11), 1258. https://doi.org/10.3390/catal11111258.

Qazi, F.; Hussain, Z.. and Tahir, M. N. (2016) Advances in Biogenic Synthesis of Palladium Nanoparticles. *RSC Advances*, *6* (65), 60277–60286. https://doi.org/10.1039/c6ra11695g.

Rajam, K.; Rajendran, S. and Saranya, R.(2012) Allium Sativum (Garlic) Extract as Nontoxic Corrosion Inhibitor. *Journal of Chemistry*, *2013*, https://doi.org/10.1155/2013/743807.

Ramesh, K. P., Singaravelu, V., Manjusri, M., A. K. Mohanty, N. Satyanarayana (2012) Soybean (Glycine max) Leaf Extract Based Green Synthesis of Palladium Nanoparticles *Journal of Biomaterials and Nanobiotechnology*, 3, 14-19 https://dx.doi.org/10.4236/jbnb.2012.31003

Sakata, Y.; Yoshida, S.; and Takamitsu, H..(2021) Synthesis of Azidoanilines by the Buchwald–Hartwig Amination. *Journal of Organic Chemistry* **2021**, *86* (21), 15674–15688. https://doi.org/10.1021/acs.joc.1c02251.

Saldan, I.; Semenyuk, Y.; Marchuk, I. and Reshetnyak, O. (2015) Chemical Synthesis and Application of Palladium Nanoparticles. *Journal of Materials Science*, *50* (6), 2337–2354. https://doi.org/10.1007/s10853-014-8802-2.

Sepideh, T; Hallajian, S.; Yasaman P. Hamedani; Nazari, P.; Darvishi, K. and Malak Hekmati. (2018)Green Synthesis of Pd Nanoparticles Mediated by Thymbra Spicata Leaves Extract and Its Application as a Recyclable Nanocatalyst for Reduction of 4-Nitrophenol and Suzuki Reactions. *Journal of Inorganic and Organometallic Polymers and Materials* , *28* (3), 1001–1010. https://doi.org/10.1007/s10904-017-0775-6.

Shafey, A. M. E.(2020) Green Synthesis of Metal and Metal Oxide Nanoparticles from Plant Leaf Extracts and Their Applications: A Review. *Green Processing and Synthesis*, *9* (1), 304–339. https://doi.org/10.1515/gps-2020-0031.

Shaik, M.; Ali, Z.; Khan, M.; Kuniyil, M.; Assal, M.; Alkhathlan, H.; Al-Warthan, A.; Siddiqui, M.; Khan, M. and Adil, S. (2017) Green Synthesis and Characterization of Palladium Nanoparticles Using Origanum Vulgare L. Extract and Their Catalytic Activity. *Molecules* **2017**, *22* (1), 165. https://doi.org/10.3390/molecules22010165.

Shameli, K.; Ahmad, M. B.; Jazayeri, S. D.; Shabanzadeh, P.; Sangpour, P.; Jahangirian, H. and Gharayebi, Y. (2012)Investigation of Antibacterial Properties Silver Nanoparticles Prepared via Green Method. *Chemistry Central Journal*, *6* (1). https://doi.org/10.1186/1752-153x-6-73.

Shankar, S. S.; Rai, A.; Ankamwar, B.; Singh, A.; Ahmad, A. and Sastry, M. (2004) Biological Synthesis of Triangular Gold Nanoprisms. *Nature Materials*, *3* (7), 482–488. https://doi.org/10.1038/nmat1152.

Sheny, D. S; Philip, D. and Mathew, J. (2012) Rapid Green Synthesis of Palladium Nanoparticles Using the Dried Leaf of Anacardium Occidentale. *Spectrochimica Acta Part A Molecular and Biomolecular Spectroscopy*, *91*, 35–38. https://doi.org/10.1016/j.saa.2012.01.063.

Sherwood, J.; Clark, J. H.; Fairlamb, I. J. S. and Slattery, J. M.(2019) Solvent Effects in Palladium Catalysed Cross-Coupling Reactions. *Green Chemistry*, *21* (9), 2164–2213. https://doi.org/10.1039/c9gc00617f.

Stephen, A. J.; Rees, N. V.; Mikheenko, I. P. and Macaskie, L. E. (2019) Platinum and Palladium Bio-Synthesized Nanoparticles as Sustainable Fuel Cell Catalysts. *Frontiers in Energy Research* **2019**, *7*. https://doi.org/10.3389/fenrg.2019.00066.

Tao, R.; Ma, X.; Wei, X.; Jin, Y.; Qiu, L. and Zhang, W.(2020) Porous Organic Polymer Material Supported Palladium Nanoparticles. *Journal of Materials Chemistry A*, *8* (34), 17360–17391. https://doi.org/10.1039/d0ta05175f.

Van Vaerenbergh, B.; Lauwaert, J.; Vermeir, P.; Thybaut, J. W.; and De Clercq, J. (2020) Towards High-Performance Heterogeneous Palladium Nanoparticle Catalysts for Sustainable Liquid-Phase Reactions. *Reaction Chemistry & Engineering***2020**, *5* (9), 1556–1618. https://doi.org/10.1039/d0re00197j.

Veisi, H.; Adib, M.; Karimi-Nami, R.; Yasaei, Z.; Tajik, M.; Mosavat, T. S.; Hemmati, S. and Suzuki–Miyaura (2017)Coupling Catalyzed by Palladium Nanoparticles Biosynthesized Using *Glycyrrhiza Glabra* as Reducing and Stabilyzing Agent. *Applied Organometallic Chemistry*, *32* (3). https://doi.org/10.1002/aoc.4138.

Veisi, H.; Faraji, A. R., Hemmati, S. and Gil, A. (2015)Green Synthesis of Palladium Nanoparticles Using Pistacia Atlantica Kurdica Gum and Their Catalytic Performance in Mizoroki-Heck and Suzuki-Miyaura Coupling Reactions in Aqueous Solutions. *Applied Organometallic Chemistry*, *29* (8), 517–523. https://doi.org/10.1002/aoc.3325.

Veisi, H.; Ghorbani-Vaghei, R.; Hemmati, S.; Aliani, M. H.; and Ozturk, T.(2014) Green and Effective Route for the Synthesis of Monodispersed Palladium Nanoparticles Using Herbal Tea Extract (Stachys Lavandulifolia) as Reductant, Stabilizer and Capping Agent, and Their Application as Homogeneous and Reusable Catalyst in Suzuki Couplin. *Applied Organometallic Chemistry* , *29* (1), 26–32. https://doi.org/10.1002/aoc.3243.

Zhao, X.; Chang, Y.; Chen, W.-J.; Wu, Q.; Pan, X.; Chen, K.; and Weng, B.(2021) Recent Progress in Pd-Based Nanocatalysts for Selective Hydrogenation. *ACS Omega*, *7* (1), 17–31. https://doi.org/10.1021/acsomega.1c06244.

Zhaq, Q.; Yu, H.; Hu, D.; Li, L.-L.; Jin, J.; Ai, M.-J.; Wei, J.; and Song, K.(2022) Recent Advances in Electrochemical Sensors Based on Palladium Nanoparticles. *Chinese Journal of Analytical Chemistry* , *50* (11), 100144. https://doi.org/10.1016/j.cjac.2022.100144.